

Supplementary Material

The role of human ventral visual cortex in motion perception

Gilaie-Dotan S, Saygin AP, Lorenzi L, Ryan Egan, Rees G & Behrmann M

Case descriptions: Additional details

Left hemisphere lesions

EL case description

EL (see Figure 3 A-D for lesion delineation and Tables 1 and 5 for case description details) has participated in many previous studies, which provide detailed description of her abilities and impairments (Behrmann et al., 1998; Behrmann and Plaut, 2012; McKeef and Behrmann, 2004; Montant and Behrmann, 2001; Mycroft et al., 2009). Briefly, previous testing revealed that she has pure alexia as well as some difficulty in object recognition.

GB case description

GB (see Figure 3 E-G for lesion delineation and Tables 1 and 5 for basic case description details) also suffers from pure alexia and, although she has not undergone extensive perceptual testing, all indications are that she has some mild impairment in object recognition, too.

Right hemisphere lesions

We provide more neuropsychological description for these cases who evince the impairment in motion perception.

SM case description

SM was 37 years old at the time of testing. He sustained a closed head injury in a motor vehicle accident at the age of 18 and recovered well after rehabilitation, aside from a persisting visual agnosia and prosopagnosia. Recent imaging (Konen et al., 2011) has located the lesion in a circumscribed region in the posterior portion of the right lateral fusiform gyrus, and the lesion is comprised of a volume of 990 mm³.

Further details of his medical and neuropsychological history can be found in previous studies (Behrmann and Kimchi, 2003; Behrmann and Plaut, 2012; Gauthier et al., 1999; Marotta et al., 2001; Nishimura et al.) and his lesion is shown in Figure 3G. SM performs within the normal range on tests of low-level visual processing and shows normal color vision.

SM's object agnosia is evidenced by his object-naming performance in the Boston Naming Test (66% correct; normal: 96.4%) and his mean reaction time per correct item (2.14 s; normal: 0.88 s). When he fails to recognize an object, he does not appear to possess any semantic or action information about this object. His auditory identification of objects is unaffected and he can provide detailed definitions in response to the auditory label of an item that he missed when it was presented visually. SM's prosopagnosia is indicated by his impaired performance in the Benton Facial Recognition Test (36/54; normal 41-54). He is unable to recognize pictures of any

famous people, despite being able to provide a good verbal identification when presented with their names auditorily. SM works in a photography studio.

CR case description

CR was 31 years old at the time of testing. He suffered from a right temporal lobe abscess with a complicated medical course including a history of Group A toxic shock syndrome, pneumonia, cardiac arrest, candida bacteremia, and metabolic encephalopathy in May 1996, approximately 15 years prior to his participation in this study. MR scans reveal a right temporal lobe lesion consistent with acute micro-abscesses of the right temporal lobe and medial occipital lobe (see Figure 3G). CR has no visual field deficits and performs within the normal range on all tests of low-level visual processing (judging size, length, and orientation of stimuli) as well as on the BORB subtests that require matching of objects from different viewpoints or along a foreshortened axis. CR is impaired at recognizing some common familiar objects, as evident by his poor recognition scores of 46/60 (76.6% correct) on the Boston Naming Test and 149/185 on the Snodgrass and Vanderwart black-and-white line drawings. His ability to recognize static living things (64%) was worse than for static nonliving things (89%). CR's performance on tests of face recognition is in the "severely impaired" range on the Benton Facial Recognition tests (scores of 36/54 and 37/54 on two separate administrations of the test). CR has participated in several previous studies (Behrmann and Williams, 2007; Behrmann and Plaut, 2012; Gauthier et al., 1999; Marotta et al., 2001) that highlight his use of part-based recognition mechanisms. CR completed community college and now runs a restaurant.

EC case description

EC, a 48-year old female, was tested four years after suffering an infarction. The radiology report states that there is low attenuation at the right temporal lobe and right occipital lobe posteriorly, consistent with a right PCA infarct (see Figure 3G). She showed difficulties in both face and object recognition on screening tests conducted prior to these experiments. She was unavailable for further testing and did not complete the motion coherence experiment.

Motion Coherence: Additional details

We note further that the right hemisphere patients started their practice with an easier coherence threshold than did the left hemisphere patients (SM at 90% and CR at 80%, vs. GB and EL at 70%), and, in spite of this, they still failed to perceive the motion coherence interval normally. Since SM finished his practice run with a final coherence of 44.78%, his starting coherence threshold was 50%, similar to controls and to GB and EL. He did not however manage to improve during the motion coherence runs, and on the contrary, finished the first run at >62% and the second at 70.57% coherence thresholds. CR finished his practice at >85% and that is why his first run started with that same threshold, his second run with 77.16% coherence. The lack of threshold improvement is not due to the initial starting threshold, as three controls who also started their practice runs with an easier opening threshold of 90% (like SM) finished their practice with thresholds of 18.4%, 20.8%, and 47.4%.

We also performed comparisons between patients and different aged controls to rule out possibilities of age affecting the results. To further examine the performance of the left hemisphere patients, we compared the performances of 61 y.o. EL and 70 y.o. GB with the performance of 8 young controls (aged 31 ± 3.1), revealing normal performance ($t_{\text{crawford}}(7) < 0.25$, $p > 0.8$). For CR (31 y.o.) and SM

(37 y.o.), we compared their performances to older controls (aged 48.3 ± 3.2) and their thresholds were at or close to significantly worse than the controls (CR: $t_{\text{crawford}}(2) = 3.44$, $p = 0.074$, SM: $t_{\text{crawford}}(2) = 5.24$, $p = 0.034$). We also compared each patient's performance to all the controls combined ($n=13$). According to this comparison too, EL and GB's performance was normal ($|t|'s < 0.25$, $p's > 0.8$), while both CR and SM's performance was significantly impaired (CR: $t(12)=4.14$, $p = 0.0014$, SM: $t(12) = 6.13$, $p=5.12 \cdot 10^{-5}$). We also checked whether there were any age effects related to the coherence thresholds, and found no correlation between age and threshold for the controls $p > 0.96$. These comparisons provide further support that the profile of normal performance revealed by the left ventral visual patients, and that of abnormal performance revealed by the right ventral visual patients is not a function of the age of the comparison group.

Motion Coherence: Additional control paradigms

Our motion coherence paradigm consisted of target motion, directed upward or rightward, that was embedded in noise dots moving in random directions. To confirm that the rightward target motion component in our paradigm did not confound the hemispheric asymmetry results we found, we conducted detailed separate unidirectional motion coherence threshold measurements for upwards, downwards, rightwards, and leftwards motion, following precisely the same thresholding procedure as in our original paradigm.

The stimuli were as in our original paradigm, but the target motion in each run was consistently moving in one (of four) directions, and the participants (patients and controls) were notified about that direction in advance of each block of trials.

The testing procedures for each motion direction followed those of our original paradigm. For all participants, motion coherence thresholds were measured for upwards motion first, then rightwards, leftwards, and downwards motion. Each motion direction began with a practice block (starting threshold of 0.9), which was followed by one or two full experimental blocks of 48 trials each. The practice of the upwards motion was a full experimental block of 48 trials, as it was meant to familiarize the participants with the paradigm at the outset. Several practice trials were provided at the beginning of each block to familiarize participants with the new direction of motion to be tested.

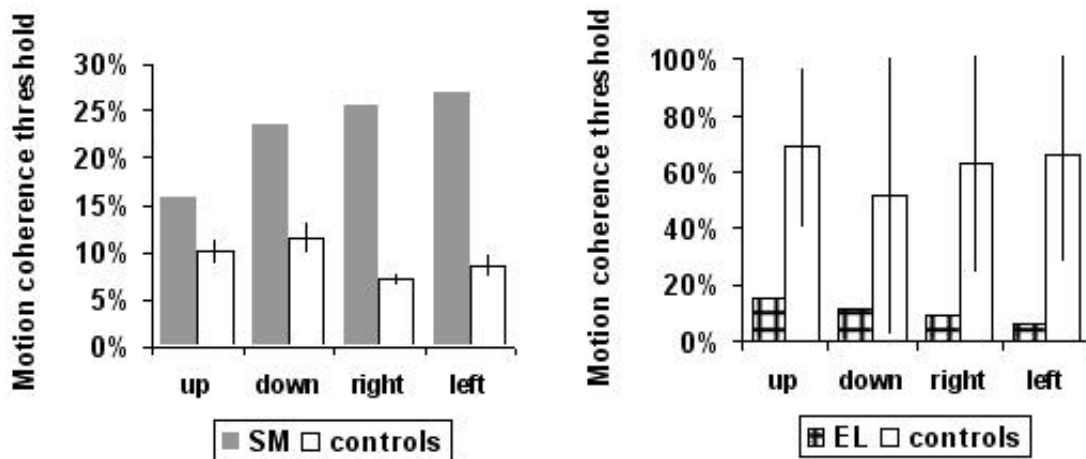
Participants

To examine whether the rightward motion component in our original paradigm affected the motion perceptual threshold measurements, we needed to determine whether (a) a lesion to right ventral cortex impairs motion coherence thresholds for leftwards motion as it does for rightwards motion (as observed in our original paradigm) and (b) motion coherence thresholds are unaffected following left ventral lesion for leftwards motion as they were unaffected for rightwards motion. To explore these two complementary findings, we tested patient SM (age 38 at the time of testing) and four age and gender matched controls (men aged 39 ± 2.9 s.d.), and patient EL (age 62 at the time of testing) and two age and gender matched controls (women aged 65 ± 1.5 s.d.) in these additional, motion coherence control experiments.

Results

SM's motion coherence thresholds were significantly impaired in all directions as displayed in Supplementary Figure 1 below (rightwards: 25.29% vs. $7.26\% \pm 0.6\%$

for controls, $t_{\text{crawford}}(3) = 24.7$, $p < 0.0009$, leftwards: 26.95% vs. $8.7\% \pm 1.3\%$ for controls, $t_{\text{crawford}}(3) = 12.15$, $p < 0.004$, upwards: 15.72% vs. $10.1\% \pm 1.4\%$ for controls, $t_{\text{crawford}}(3) = 3.55$, $p < 0.04$, downwards: 23.48% vs. $11.59\% \pm 1.7\%$ for controls, $t_{\text{crawford}}(3) = 6.02$, $p < 0.02$). EL's motion coherence thresholds were unaffected by her left ventral visual lesion, and her performance was not significantly different from that of her controls in all directions (rightwards: 9% vs. $63\% \pm 38\%$ for controls, $t_{\text{crawford}}(3) = -1.15$, $p = 0.23$, leftwards: 6.3% vs. $66\% \pm 38\%$ for controls, $t_{\text{crawford}}(3) = -1.29$, $p = 0.21$, upwards: 15.9% vs. $68.9\% \pm 28.3\%$ for controls, $t_{\text{crawford}}(3) = -1.53$, $p = 0.184$, downwards: 11.4% vs. $52\% \pm 49.2\%$ for controls, $t_{\text{crawford}}(3) = -0.67$, $p = 0.31$).



Supplementary Figure 1: Motion coherence thresholds for four different directions for SM, EL, and their matched controls.

These additional motion coherence results confirm our original findings that right ventral visual lesion causes impairments in motion coherence thresholds, and rules out the possibility that the original results were biased by the rightward motion component in our original paradigm. Furthermore, these results confirm our original findings that a lesion to right, but not left ventral, cortex impairs motion coherence

thresholds. Specifically, SM's motion coherence thresholds were impaired in all directions whereas EL's thresholds were unimpaired in all directions.

Motion Coherence: Lapse rates analysis

Lapse rates measure the rate at which observers make stimulus-independent errors, and, thus, can be measured as the error rate at the tail end of the psychometric function, where ceiling performance is expected. Since the motion coherence was a threshold estimation experiment, it is not as simple to measure lapse rates as the stimulus intensity constantly changes. Nevertheless, when we examined the error rates at high coherence levels, for GB and EL, accuracy was at 100% corresponding to lapse rates of 0. For SM, in the control paradigm when all coherent stimuli were at the same direction throughout the run, his lapse rate was 0 (no errors at high intensities of coherence). For CR, when he felt confident with the task his lapse rate (at high coherence levels) was 0 (no errors, except for the 1st trial in that session, which could be due to the beginning of the session) for thresholds above 55% coherence (9 trials). Thus, it is highly unlikely that the motion coherence thresholds of SM and CR are due to lapse rates. Instead, they seem to genuinely reflect their motion coherence impaired thresholds.

Motion Detection: Additional details

To verify that the observed patterns of normality and impairment were not dependent on age effects, we carried out further comparisons, pitting the patient performance against that of control groups of various ages. We conducted a stringent test of the normality of motion detection in patients with left hemisphere lesions by comparing the performances of 61 y.o. EL and 70 y.o. GB with that of 11 young controls

(controls selected for CR; aged 31.4 ± 3.2). Given that EL and GB scored 100% accuracy as did all the young controls, the older patients and young controls have equivalent scores (for EL and GB: $t_{\text{crawford}}(10) \approx 0$, $p \approx 1$). To assess the extent of the impairment (relative to age-matched controls) for CR (31 y.o.), SM (37 y.o.), and EC (48 y.o.), we compared their very slow motion detection performance to that of older controls (aged 63 ± 3.6). All three patients' thresholds were significantly impaired even under these conditions (for CR, SM, and EC: $t_{\text{crawford}}(3) < -10^5$, $p < 10^{-13}$). We also compared the reaction times of the motion detection task for each patient vs. all the controls, and found that the left ventral patients GB and EL, were completely normal in their reaction time ($t(26)$'s < 0.8 , p 's > 0.45), while the right ventral patients were all significantly slower than the controls (CR, SM, EC : p 's < 0.04 , $t(26) > 2.29$). We also examined whether there were any age effects on the RTs and found that there was no correlation between age and reaction times $r=0.09$ $t(25) = 0.451$, $p > 0.65$. Furthermore, the mean RT (1/3 youngest controls) = 3.95s, while mean RT(1/3 oldest controls) = 3.82s. These comparisons provide further support for the claim that the results we obtained were not merely a function of the age of the control group enlisted; the intact performance of the left ventral visual patients, and the impairment in detecting of slow motion in the right ventral visual patients hold even under a wide range of statistical comparisons.

3D structure-from-motion recognition: Additional details

In the same manner detailed above for motion coherence and motion detection, we also performed statistical comparisons for the patients against different aged controls. CR and SM were compared to older controls (aged 48.2 ± 3.5), and here too they were significantly impaired even when compared to these older controls (CR:

$t_{\text{crawford}}(8) = -3.68$, $p = 0.0062$, SM: $t_{\text{crawford}}(8) = -2.63$, $p = 0.03$). On the other hand, the older patients, EL and GB, scored within the normal range even when compared to younger (aged 31.4 ± 3.2) controls (EL and GB: $t_{\text{crawford}}(10) = 0.52$, $p = 0.62$).

Lesion tracing criteria

For EL, since the average intensity values varied across each structural image regardless of the lesion (e.g. between anterior and posterior regions, or right and left hemispheres), the definition of the lesioned tissue was not based only on absolute intensity values. Instead, the definition of the lesioned tissue also took into account abrupt local changes in intensities between lesioned and adjacent healthy tissue, and continuity of abnormal lesioned tissue. Locally, lesioned tissue always had substantially lower values of intensity than healthy tissue. In most parts of EL's brain and around the lesion, healthy tissue intensity values ranged from 200 to above 350 (a.u.), while lesioned tissue intensity values ranged from 54 to 170. However, in specific locations 170 was considered healthy tissue (adjacent to value of 117 of a lesioned tissue). We provide lesion size estimates based on local intensity variations and continuity assessment, and also a more conservative estimation based on intensity values <150 in the predefined lesion zone (see Table 5).

With SM's structural images, we also faced the issue of local variations in intensity values; thus, as with EL, we delineated the lesion based on intensity values, continuity of the lesioned tissue, and abrupt changes in local intensity values between the lesion and adjacent healthy tissue. Common values for healthy tissue were above 200 to even above 350, however, locally healthy tissue could have value of 171. Lesioned tissue typically had values ranging from as low as 60's to values around 150, however,

locally, values of 160 or 174 could be attributed to lesioned tissue. We provide the lesion size estimate according to the criteria laid out above, along a conservative estimate for lesion when lesioned intensities < 160 .

Since CR's lesion is of a different etiology than that of EL and SM, the lesion delineation criteria were different. On top of a medial right temporal lobe hemorrhage, there are foci of petechial hemorrhage seen along the grey/white junction at multiple areas that appear as a very dark centre (intensity values of below 35) bordered by very bright intensity tissue (intensity above 120). Healthy tissue in CR's structural images had intensity values of 55-95. Furthermore, CR has a definitive lesion in the right temporal lobe (see above) that is evident and confirmed by an expert neuroradiologist in the past and during the current study. There are, however, some suspicious hyperintensities in the left hemisphere (perhaps resolved abscesses) and so we adopt a conservative approach here and leave open the possibility of additional left hemisphere insult. Critical for our case, however, the lesion impinged on the ventral aspects of the right hemisphere (see Figure 3G), but did not overlap the expected locations of R/L-MT/V5. Of relevance too is that CR did not have a visual field defect.

Lesioned tissue in GB's and EC's original clinical structural images were used to guide delineation in normalized MNI. GB's original DICOM images were loaded into MATLAB (Mathworks, Natick, MA, USA) where intensity values of lesioned tissue were above 0.5, while healthy tissue intensity values were below 0.4. Due to technical issues with MATLAB reading EC's DICOM images, EC's structural images were loaded into MicroDicom (<http://www.microdicom.com/>) and then exported to bitmap images. Typically lesioned tissue intensity values were below 105, while healthy

tissue values were above 110. In the lesion delineation process we also took into account (as with the other patients) continuity of the lesioned tissue, and abrupt intensity changes between the lesion and adjacent healthy tissue. After the lesion tracing in the original images detailed above, an approximated corresponding delineation was carried out onto a single subject T1 SPM MNI-normalized template (as illustrated in Figure 3 E, F).